The Polar Deposits of Mars

Shane Byrne

Lunar and Planetary Laboratory, University of Arizona, Tucson, Arizona 85745;
email: shane@lpl.arizona.edu

Annu. Rev. Earth Planet. Sci. 2009. 37:535–60

First published online as a Review in Advance on January 15, 2009

The *Annual Review of Earth and Planetary Sciences* is online at earth.annualreviews.org

This article's doi:
10.1146/annurev.earth.031208.100101

0084-6597/09/0530-0535$20.00

Key Words

martian, ice, climate, stratigraphy, geology, glaciology

Abstract

The tantalizing prospect of a readable record of martian climatic variations has driven decades of work toward deciphering the stratigraphy of the martian polar layered deposits and understanding the role of the residual ice caps that cover them. Spacecraft over the past decade have provided a massive infusion of new data into Mars science. Polar science has benefited immensely due to the near-polar orbits of most of the orbiting missions and the successful landing of the Phoenix spacecraft in the northern high latitudes. Topographic, thermal, radar, hyperspectral, and high-resolution imaging data are among the datasets that have allowed characterization of the stratigraphy of the polar layered deposits in unprecedented detail. Additionally, change within the residual ice caps has been monitored with spacecraft instruments for several years. These new data have provided a golden opportunity to understand the interplay between the martian orbit, climate, and polar ice.

INTRODUCTION

In many respects, Mars is an Earth-like planet. Nowhere is this statement both more and less true than in its polar regions. Mars and Earth share large, kilometers-thick sheets of water ice (**Figure 1**) that interact with the planetary atmosphere and record climatic variations in their stratigraphy. Earth and Mars both undergo Milanković cycles that have profound effects on the distribution of stable ice, and the familiar processes of glacial flow and volcanism can affect ice on both bodies, albeit at different rates. However, the opening statement is also false in many ways. Terrestrial ice caps have important oceanic interactions not present on Mars. Mars has seasonal ice caps of CO_2 ice that condense out an appreciable fraction of the planetary atmosphere. Parts of these caps anneal into transparent slabs before sublimating and producing geyser-like effects

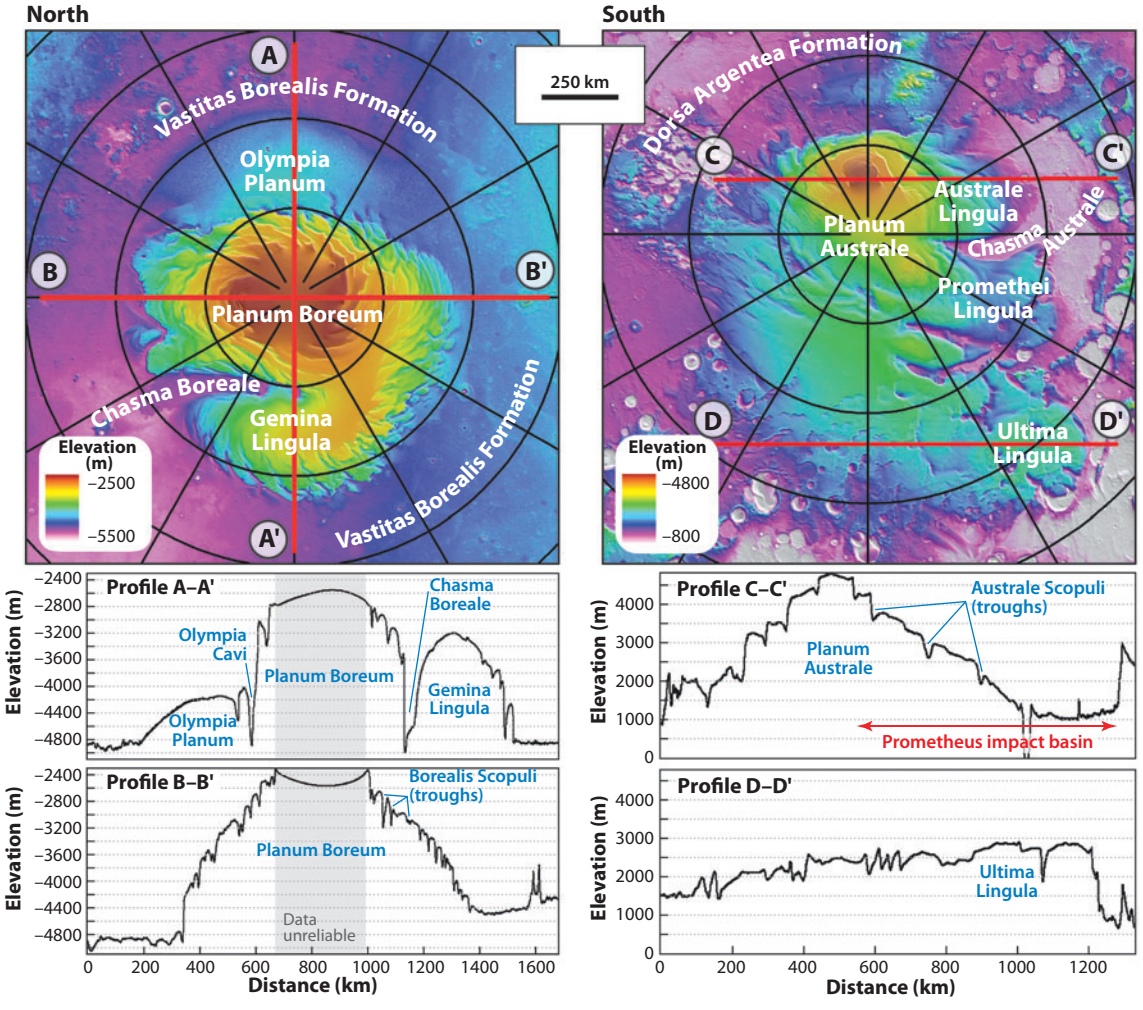

Figure 1

Regional MOLA topographic maps showing the north (*left*) and south (*right*) polar regions at the same scale. Red lines indicate locations of topographic profiles. Gray shading in north polar profiles indicates the region for which topographic data are unreliable. Parallels are plotted every 5°. 0°E is at the bottom in the north polar view and at the top in the south polar view.

Table 1 Acronyms

Missions and instruments		
Mars Reconnaissance Orbiter (MRO)	CRISM	Compact Reconnaissance Imaging Spectrometer for Mars (Murchie et al. 2007a)
	HiRISE	High Resolution Imaging Science Experiment (McEwen et al. 2007)
	SHARAD	Mars Shallow Subsurface Radar (Seu et al. 2007b)
Mars Express (MEX)	MARSIS	Mars Advanced Radar for Subsurface & Ionosphere Sounding (Nielsen 2004)
	OMEGA	Observatoire pour la Minéralogie, l'Eau, les Glaces, et l'Activité (Bibring et al. 2005)
Mars Global Surveyor (MGS)	MOC	Mars Orbiter Camera (Malin & Edgett 2001)
	MOLA	Mars Orbiter Laser Altimeter (Smith et al. 2001)
	TES	Thermal Emission Spectrometer (Christensen et al. 2001)
Mars Odyssey (M01)	THEMIS	Thermal Emission Imaging System (Christensen et al. 2004)
Polar geologic units		
North	NRIC	Northern residual ice cap
	NPLD	North polar layered deposits
	BU	North polar basal unit
South	SRIC	Southern residual ice cap
	SPLD	South polar layered deposits
	DAF	Dorsa Argentea Formation

and a host of features alien to terrestrial experience. Thus, the polar deposits of Mars represent a unique blend of the familiar and the exotic that often confounds and always fascinates.

The current polar deposits consist of several icy bodies that respond to the martian environment over different timescales. The seasonal CO_2 ice caps exist for only a fraction of a martian year, and their behavior is closely coupled to present-day meteorology. The northern residual ice cap (NRIC) and the southern residual ice cap (SRIC) are stable features (at least over centuries), and their history is a key constraint on the interannual variability of the current climate. The north and south polar layered deposits (NPLD and SPLD, respectively) are layered domes of dusty water ice several kilometers thick that record climatic variation, probably over timescales of 10^5 to 10^9 years, in a similar way to terrestrial ice caps. Older polar deposits, stratigraphically beneath the polar layered deposists, probably reflect episodes in martian history with environments quite different from that of today.

Contemporaneous with the initial exploration of the martian poles (Murray et al. 1972), it was realized that quasi-periodic variations in insolation due to variations in the orbital eccentricity (Murray et al. 1973) and planetary obliquity (Ward 1973) have occurred and are likely to have had profound effects on the martian climate. Although a definitive link between polar stratigraphy and orbital variations remains elusive, data from a recent string of successful missions have brought us closer to making this important connection than ever before.

Missions and instruments are referred to by acronyms defined in **Table 1**, and the reader is referred to references in that table for a full description of the capabilities of these hardware. Coordinates quoted herein use planetocentric latitudes and east longitudes relative to the IAU 2000 datum (Seidelmann et al. 2002). Seasonal dates are quoted as aerocentric longitude of the Sun in degrees (L_s).

This is by no means an exhaustive survey of the discoveries produced in this field. As with all reviews, compromises have been made in both scope and depth in an attempt to balance the two. Chief among these has been the exclusion of new discoveries related to the seasonal ice caps. For

example, although dominated by CO_2 ice (Leighton & Murray 1966), the northern seasonal ice cap is now known to have an annulus of water frost that tracks its outer edge (Kieffer & Titus 2001, Wagstaff et al. 2008). In contrast, water frost is patchier (Titus 2005), when present at all, in the southern cap. Large portions of the southern seasonal CO_2 ice cap have been shown to sinter into solid transparent slabs that sublimate from the bottom up, driving the pressurized release of CO_2 jets that can erode the surface and deposit debris fans (Kieffer 2000, 2007; Kieffer et al. 2006). In contrast, mass and thickness measurements indicate that other portions of the seasonal caps may form with porosities approaching 70% (Aharonson et al. 2004, Haberle et al. 2004). Unfortunately, a discussion of these phenomena cannot be accommodated in this review, and the reader is referred to Titus et al. (2008a), which focuses on these deposits and processes.

Mars polar science has benefited enormously from a series of four conferences, held over the past decade, dedicated to this subject. The proceedings of these conferences are summarized in special issues of Icarus (Clifford et al. 2000, 2001, 2005; Fishbaugh et al. 2008a), and the interested reader is referred to these volumes and that of a special issue of Planetary and Space Science (Titus et al. 2008b) for the full discussion of many of the results summarized here. This review focuses on recent advances. A comprehensive summary of Mariner and Viking mission data and investigative results can be found in Thomas et al. (1992).

RESIDUAL ICE CAPS

South Polar Residual Ice Cap

Retreat of the seasonal CO_2 ice caps during the summer reveals bright residual ice caps that persist all year. The SRIC is composed of high-albedo solid CO_2 (Kieffer 1979). It is on the order of a few meters thick (Byrne & Ingersoll 2003a, Tokar et al. 2003, Prettyman et al. 2004) and has areas at its margins and in its interior where the underlying water ice of the SPLD shows through (Titus et al. 2003, Bibring et al. 2004, Hansen et al. 2005). Montmessin et al. (2007) have linked the deposition of this water ice to the most recent reversal of the argument of perihelion. Under current conditions, the SRIC exists in a precarious position in which its stability critically depends on its ability to maintain a high albedo (Jakosky & Haberle 1990). If terrain at this latitude were to become defrosted, then solar heat could be stored in the subsurface, which would offset condensation of CO_2 frost the following winter and ensure full defrosting each subsequent year. Once thought to be a large reservoir of CO_2 capable of buffering climate change, it is now known that the SRIC contains, at most, the equivilant of only a few percent of the current atmospheric reservior (Byrne & Ingersoll 2003a).

High-resolution imagery (Thomas et al. 2000) shows a wide range of morphologies on the SRIC, ranging from flat-floored, quasi-circular pits (the features of which are dubbed Swiss cheese features) (**Figure 2*a***) to linear ridges (dubbed fingerprint terrain) (**Figure 2*c***). The pits come in a range of sizes and morphologies and are embedded in CO_2 ice slabs that vary in thickness from 2 to 10 meters. The thicker ice slabs have been heavily eroded (in most places, only isolated mesas remain) and are draped by a much more recent thin ice slab (Thomas et al. 2005). Repeated observations have shown that the inclined walls of the embedded pits retreat by several meters each year (Malin et al. 2001, Thomas et al. 2005) and that pits embedded in thick slabs expand faster (8–10 m each martian year) than those embedded in thin slabs (2–6 m each martian year). North-south asymmetries in the pit shapes (**Figure 2*a***) show that their walls expand in response to ablation (Byrne & Ingersoll 2003b). The walls of the pits in the thick ice slabs are dark relative to the high-albedo CO_2 ice on the flat interpit surfaces (Malin & Edgett 2001). As

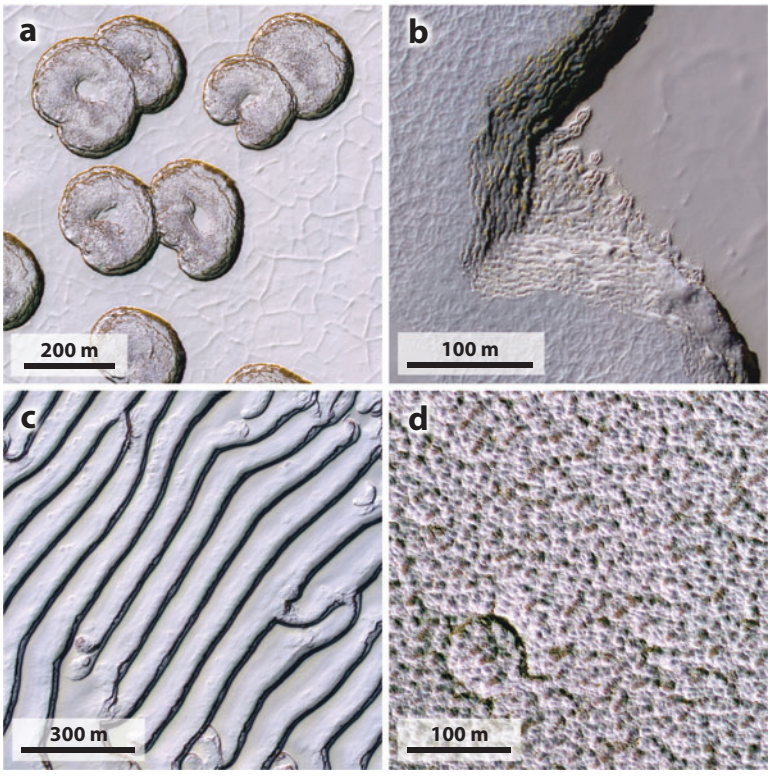

Figure 2

HiRISE false-color images of the residual ice caps. (*a*) PSP_005517_0930, at 353°E 86.9°S, showing "Swiss cheese" pits in an 8-m-thick slab of CO_2 ice. (*b*) PSP_003882_0930, at 16°E 86.7°S, showing layers within a ~10 m thick CO_2 ice mesa. (*c*) PSP_005954_0940, at 308°E 86.2°S, showing linear fingerprint terrain within the SRIC. (*d*) PSP_001922_2680, at 135°E 88°N, showing typical NRIC ice texture and a rare impact crater.

CO_2 ice must have a high albedo in order to accumulate, the low albedo of the exposures of the buried CO_2 ice may be the result of grain growth after burial rather than incorporation of dust during deposition. HiRISE observations show that the dark pit walls in the thick slabs retreat and undercut the uppermost bright layer, causing mass-wasting (Byrne et al. 2008a). Pits in thin slabs of CO_2 ice do not exhibit dark walls (perhaps because this ice is younger), which is likely why they expand more slowly, although density variations between the thick and thin ice slabs have also been invoked to explain this (James et al. 2007). Models of Bonev et al. (2008) suggest sublimation should be enhanced during years with planet-encircling dust storms, which agrees with measurements of differing pit expansion rates (Byrne et al. 2008a) in dusty years versus clear years.

The history and fate of this deposit is unknown but certainly takes place over timescales short in comparison to even the mostly rapidly varying orbital element. Multiple layers in the thicker ice slabs (Thomas et al. 2005) indicate several discrete depositional events (**Figure 2*b***). Some populations of pits have narrow distributions of size and expansion rates, indicating a common formation date (Byrne & Ingersoll 2003b) that may be tied to an event in 1969, when atmospheric water was observed above the SRIC, indicating a much reduced covering of CO_2 ice (Barker et al. 1970). Mariner 9 observed the SRIC soon afterward and found much patchier CO_2 ice

coverage than today (James et al. 2007). Piqueux & Christensen (2008) have attempted to use historical telescopic and spacecraft data to reconstruct a history of the SRIC that involves at least two major episodes of erosion. Although peripheral exposures of water ice (Titus et al. 2003) indicate that the SRIC has recently retreated in extent, changes in extent from the Mariner 9 mission to today have been minimal (Piqueux & Christensen 2008). Byrne et al. (2008a) modeled the evolution of SRIC landscapes and proposed that the SRIC can be eroded and regenerated on timescales of about 60 martian years. In this model, the formation of pits is linked to evolution of surface roughness above a critical threshold, and the cap regeneration mechanism involves episodes of enhanced atmospheric precipitation of CO_2 ice, which reduces this roughness.

The fact that the SRIC flat surfaces remain bright (i.e., fine grained) all year implies that CO_2 ice is being buried before grain growth reduces its albedo; thus, the mass-balance of these surfaces is one of net accumulation. This accumulation can offset, or perhaps overwhelm, the ablation associated with expansion of the pits. As such, it is not clear whether the SRIC is in a state of net accumulation or ablation. Expansion of these pits does not in itself indicate any secular climate change is in progress. The layers exposed (**Figure 2*b***) in the SRIC mesas likely constitute a valuable record of interannual variability of the current climatic regime.

North Polar Residual Ice Cap

The NRIC is composed of water ice (Kieffer et al. 1976). Its visible albedo is lower than what may be expected from examples of terrestrial ice, indicating either contamination with dust or large ice grains (Kieffer 1990). Recent hyperspectral observations (Langevin et al. 2005b) have resolved this ambiguity and have shown that the NRIC ice is composed of large, dust-free ice grains. The observation of large ice-grain sizes implies that old ice is being exposed during the summer, which would mean that the NRIC is currently undergoing a net loss of material. Several isolated spots remain bright (i.e., they retain their seasonal water frost) all year and thus are locations of new accumulation (Kieffer & Titus 2001, Langevin et al. 2005b, Byrne et al. 2008b, Calvin & Titus 2008). The extent of the NRIC can vary interannually (Malin & Edgett 2001, Hale et al. 2005); however, these variations are limited to a few percent of its area and are reversible on timescales of years (Byrne et al. 2008b).

At hectometer-length scales, NRIC topography is extremely smooth (Aharonson et al. 2001). However, high-resolution imagery (Thomas et al. 2000, Byrne et al. 2007) shows that the surface of the NRIC has a homogenous pitted texture (**Figure 2*d***) at length scales of 10 to 20 meters. Photoclinometry (Herkenhoff et al. 2002) and photometric modeling (Byrne et al. 2008b) indicate that this texture has a relief of less than one meter. HiRISE data (e.g., **Figure 2*d***) show the floors of the pits have a similar color to the underlying NPLD, indicating that the NRIC thickness is identical to the pit depth (Byrne et al. 2007).

The NRIC is commonly interpreted as the current site of NPLD formation; however, the NRIC can also be seen to unconformably overlie the NPLD by draping over layers exposed in the upper parts of troughs (Tanaka et al. 2008). Tanaka (2005) used two small craters (including the one shown in **Figure 2*d***) on material underlying the NRIC to infer an upper age limit of 8.7 Kyr, which corresponds with a recent downturn in north polar insolation that began ~20 Kyr ago as a result of changes in the argument of perihelion (Montmessin et al. 2007). However, Galla et al. (2008) used CTX and HiRISE data to identify and analyze 70 craters on this deposit. Statistical analysis of these craters shows that the NRIC is an equilibrium surface and cannot be characterized by a single age.

POLAR LAYERED DEPOSITS

Physical Characteristics and Composition

The topographic domes of Planum Boreum (north) and Planum Australe (south), shown in **Figure 1**, are mostly composed of the polar layered deposits (PLD); the residual ice caps that partially cover these domes are volumetrically inconsequential by comparison. The volumes of the northern and southern PLD are ~1.14 and ~1.6 million km^3, respectively (Smith et al. 2001, Plaut et al. 2007a), which together have a volume similar to that of the Greenland ice sheet (~2.6 million km^3).

MOLA data show Planum Boreum to be a quasi-circular structure ~1000 km across that rises ~3 km above the surrounding plains. Regional topographic data show that Planum Boreum lies within a broad depression that, although not officially named, is often referred to as the Borealis basin. The dome of Planum Boreum sits on top of the Vastitas Borealis Formation, which is relatively homogeneous and of early Amazonian age (Tanaka et al. 2008). Southward at 180°E, Planum Boreum is adjoined by Olympia Planum, a half-dome-shaped structure that rises ~600 m above the surrounding plains. Planum Boreum is split by the large canyon Chasma Boreale (~500 km long, 50 km wide, and 1–2 km deep; see **Figure 1**, profile A-A′), which divides a large lobe of material named Gemina Lingula from the main dome. MARSIS and SHARAD have observed the basal topography of Planum Boreum (Picardi et al. 2005, Phillips et al. 2008) and found it to be remarkably flat, indicating that the lithospheric thickness exceeds 300 km if in flexural equilibrium (Phillips et al. 2008).

Planum Australe is also a dome-like structure that is 3–4 km thick in its thickest regions (longitudes –90° to +90°E); however, it also extends equatorward in a broad, flat, lower-relief plateau in the longitude range 90°–270°E (see **Figure 1**). Planum Australe sits on top of the heavily cratered southern highlands and partially covers the Prometheus impact basin. A large canyon, Chasma Australe, cuts through Planum Australe with similar dimensions to Chasma Boreale in the northern deposits; however, in contrast to Planum Boreum, Planum Australe contains several other large canyons such as Promethei Chasma and Ultimum Chasma. MARSIS observations of the base of Planum Australe show an irregular surface (Plaut et al. 2007a) containing several large depressions near the south pole (probably impact craters) but no overall downward flexure of the lithosphere.

Both PLDs have long been thought to be composed of atmospherically deposited dust and water ice (Cutts 1973), with changes in the mixing ratio of these components producing the distinct layers. Buried CO_2 ice and CO_2 clathrate hydrate have been eliminated as important components, on the basis of thermal (Mellon 1996) and mechanical strength (Nye et al. 2000) arguments. Those portions of the PLDs not covered by the residual ice caps have an orange-brown color (e.g., **Figure 3*a***) similar to that of dust deposits elsewhere on the planet. This color is commonly interpreted as indicating a dust lag generated by sublimation of ice-rich material (e.g., Tanaka et al. 2008). Recent hyperspectral data from the CRISM instrument have detected water ice in the layered exposures of the NPLD at the head of Chasma Boreale (Murchie et al. 2007b). MARSIS radar transparency data provide a strong constraint on the bulk composition of both PLDs and show that the northern (Picardi et al. 2005) and southern (Plaut et al. 2007a) deposits are almost pure water ice with upper limits on the volume fraction of dust of 2% and 10%, respectively. SHARAD data yield similar NPLD transparencies (Phillips et al. 2008) but do not penetrate to the base of the SPLD (Seu et al. 2007a), possibly due to a wavelength-dependent effect such as volume scattering from pervasive fracturing. An additional compositional constraint comes from the density of the SPLD, which has been derived from analysis of the gravitational anomaly

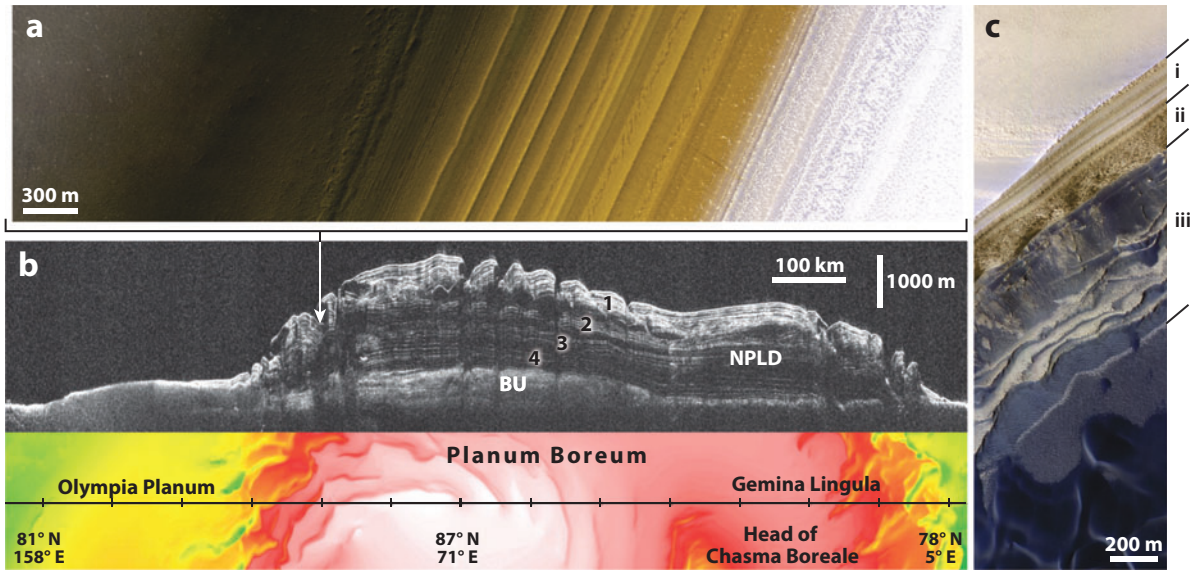

Figure 3

North polar stratigraphy from HiRISE imaging and SHARAD radar. (*a*) HiRISE false-color image PSP_008936_2660, at 144°E 86°N, showing typical exposures of layers in trough (*downhill*, *left*) also covered by radargram. (*b*) Radargram from SHARAD orbit 5192 with associated ground track. Time-to-depth conversion assumed a subsurface permittivity of three. Reproduced from Phillips et al. (2008) with permission from AAAS. Location of trough shown in (*a*) is indicated. (*c*) HiRISE false-color image PSP_001593_2635, at 119°E 83.4°N, showing scarp with transition in layering from smooth (*i*), to polygonally fractured (*ii*), to the sand-rich basal unit (*iii*).

associated with Planum Australe. Independent analysis by Zuber et al. (2007) and Wieczorek (2008) derived remarkably consistent bulk densities of 1220 and 1271 Kg m^{-3}, respectively. The volume fraction of dust to which this corresponds depends on the density one chooses for the dust itself, but it is likely ~15%. Although both PLDs are dominated by water ice, the reported dust values for the SPLD are, so far, consistently higher.

Although the bulk composition of the PLDs are becoming better constrained, considerable uncertainty remains about compositional variation from layer to layer. Individual reflections in the SHARAD data are apparent (**Figure 3*b***) and may come from layers or packets of layers in visual datasets. Phillips et al. (2008) use the approach of Nunes & Phillips (2006) to constrain the relationship between a SHARAD reflection and composition. The thinnest layers of the NPLD visible in the HiRISE data are ~10 cm thick (Herkenhoff et al. 2007). For SHARAD to detect a reflection from such a layer, it would have to be comprised of at least 10% dust. Lower dust concentrations are possible for thicker layers, e.g., 2% for a 1 m–thick layer.

Both PLDs are incised with troughs and scarps, which exhibit a spiraling planform (**Figure 1**) and expose interior layers (e.g., **Figure 3*a***). It is likely that their formation mechanism is related to a feedback effect between slope and ablation (Howard 1978). Several innovations on this model have appeared to explain the spiral pattern. Fisher (1993) combined ablation with asymmetric ice flow to produce spiral forms. Pelletier (2004) included the effects of lateral heat flow (although the importance of this process is questionable) and showed that spiral forms can self-organize. Ng & Zuber (2006) considered a spatial instability whereby moisture in air blowing away from the pole is deposited on bright surfaces and replenished by ablation from dark surfaces. These dark surface elements can then develop into troughs via the ablation mechanism. The Ng and Zuber model is attractive in that coriolis deflection of the wind produces troughs that spiral in the opposite sense,

as observed. Once formed, troughs and scarps are modified by aeolian (Howard 2000, Rodriguez et al. 2007) and mass-wasting (Murray et al. 2001, Herkenhoff et al. 2007) processes. Russell et al. (2008) observed new debris at the base of several NPLD scarps, indicating that mass-wasting is ongoing.

Two main theories have been advanced to explain the origins of the large PLD reentrants of Chasmas Australe and Boreale. In one, sub-PLD melting (likely from volcanic heating) and catastrophic outflow of meltwater carves the canyon (Clifford 1987), and in the other, downslope funneling of katabatic winds, coupled with ablation of steep surfaces, enlarges some small seed-feature (Howard 2000). Recent analyses have favored the outflow explanation for Chasma Boreale (Benito et al. 1997, Fishbaugh & Head 2002, Greve 2008) and for Chasma Australe (Anguita et al. 2000), although most also suggest postformation aeolian modification. However, the analysis of Warner & Farmer (2008a) supports a predominantly aeolian formation mechanism, and Tanaka et al. (2008) see no evidence for outflow channel features on the ancient floors of the Chasma Boreale head scarps and thus favor formation via ablation and aeolian and mass-wasting processes. In addition, Planum Boreum is far from any obvious volcanic constructs, with a regionally thicker lithosphere than anticipated (Phillips et al. 2008). Cone-like features at the periphery of Planum Boreale (Abalos Colles), originally thought to be volcanic (Garvin et al. 2000), are now interpreted as eroded remnants of a former extent of the lowermost unit of Planum Boreum (Tanaka et al. 2008, Warner & Farmer 2008b). Radar data have shown no evidence for current melting at the base of either PLD.

Stratigraphy and Age

Tanaka et al. (2008) have mapped the Planum Boreum materials into several units, including the residual ice cap and the units encompassing the north polar basal unit (BU) and sand dunes. The bulk of the classical NPLD are mapped as a single unit characterized by its laterally continuous layers, with variable brightness, roughness, and slope where exposed. MOC imaging data of NPLD layer exposures showed layering down to the limit of resolution, but this was not the case with the higher resolution HiRISE data, which have fully resolved the thinnest layers to be decimeters thick (Herkenhoff et al. 2007). PLD exposures were expected to be mantled by a lag deposit (Hofstadter & Murray 1990), and HiRISE imaging of NPLD exposures showed what appeared to be a thick mantling deposit that locally slumped (Herkenhoff et al. 2007). It is possible that exposures of thinner layers exist beneath this lag and that only the most prominent layers can protrude from the mantling deposit. SHARAD data (Phillips et al. 2008) shows that the NPLD thickness is fairly uniform (~2 km) across the interior of Planum Boreum (**Figure 3*b***). At face value, the thicknesses of the thinnest layer and of the NPLD measured by HiRISE and SHARAD, respectively, imply that there are $<10^4$ individual layers in the NPLD (although the lag deposit could mask thinner layers). The radar data show that layering within the NPLD is not constant with depth. Phillips et al. (2008) identified four finely layered packets (**Figure 3*b***) separated by zones that appear relatively massive to radar. The uppermost layered packet extends to the current surface of Planum Boreum and is ~500 m thick, which means that almost all of the troughs in the interior of Planum Boreum (such as that shown in **Figure 3*a***) expose only layers from this packet as earlier inferred by stratigraphic correlations (Milkovich & Head 2005, Fishbaugh & Hvidberg 2006). In contrast, steep scarps near the periphery of Planum Boreum (**Figure 3*c***) expose sections of layering up to 1 km thick. In these locations, HiRISE images show a distinct change in layering style (Herkenhoff et al. 2007); the lower section of these exposures is steeper and exhibits extensive polygonal fracturing (**Figure 3*c,ii***), and the upper section appears similar to exposures in the troughs, with gentle slopes and a lack of fracturing (**Figure 3*c,i***). Although

currently speculative, it is possible that this morphologic distinction corresponds to the change from layered to unlayered in SHARAD data (Herkenhoff et al. 2007).

Unconformities in the NPLD are common and have been mapped from imaging datasets, e.g., Tanaka (2005). These unconformities are concentrated at the periphery of the NPLD in the Gemini Scopuli (30°–120°E), a region of complex geomorphology where different troughs and scarps crosscut each other. Examples exist of multiple angular unconformities stacked within single troughs (Tanaka et al. 2008), indicating that NPLD accumulation was punctuated by episodes of ablation, or that erosion and accumulation acted simultaneously in different regions of the NPLD. Less obvious deposit-wide unconformities have been identified as separating layer sequences with different stratigraphic properties (Milkovich & Head 2005, Fishbaugh & Hvidberg 2006).

The upper meters to decameters of the NPLD contain 6–8 darker layers that are sometimes known as banded terrain (Howard et al. 1982, Tanaka et al. 2008). A unit intermediate between this banded terrain and the NPLD (Rodriguez et al. 2007) is characterized by low albedo material that is likely to be mostly ice-free and that acts as a source for the dark veneers that partially cover the banded terrain and residual ice.

The SPLD rests upon older Hesperian and Noachian materials, including the Dorsa Argentea Formation. Layers in the SPLD seem thicker than those of the NPLD. SPLD layers in Australe Mensa were measured by Byrne & Ivanov (2004) to be several meters thick (as opposed to several decimeters in the NPLD). Exposures of SPLD layers also commonly form multiple terraces, whereas in the NPLD, layer exposures tend to remain more flush with the trough wall.

Kolb & Tanaka (2006) divide the SPLD into two units, Australe 1 and Australe 2, on the basis of a prominent deposit-wide unconformity. The lower unit, Australe 1, comprises the bulk of the SPLD, but it is mostly covered by the relatively thin (∼300 m) Australe 2 unit, except on trough and canyon walls. An exception is the region comprised of Promethei Lingula and Australe Sulci, where Australe 1 is visible on flat surfaces. In geologic mapping of this region, Kolb & Tanaka (2006) further divided the Australe 1 unit into two members separated by an angular unconformity. SHARAD radar data of Promethei Lingula (Seu et al. 2007a) show a prominent angular unconformity at the surface and in the interior of the SPLD, consistent with the findings of Kolb and Tanaka.

The internal structure of the SPLD has been investigated by combining images and topography (Byrne & Ivanov 2004, Milkovich & Plaut 2008), and with radar (Seu et al. 2007a, Milkovich et al. 2008b). Byrne & Ivanov (2004) analyzed SPLD exposures in the area of the SRIC and found that layers in that region correspond closely to a parabolic dome. Milkovich et al. (2008b) correlated layers throughout the SPLD and found that these deposits could be divided into three superposed units with different extents. Attempts to correlate SPLD radar reflections with layers in visible datasets suggest that 3–7 layers in a MOC image correspond to a single reflection in SHARAD data (Milkovich et al. 2008b). Although less apparent than in the northern deposits, SHARAD data show that layers in the SPLD are bunched into packets, the boundaries of which generate single reflections in the MARSIS dataset (Milkovich et al. 2008b).

The length of time represented by the stratigraphy of these deposits is a key but difficult question. Impact craters are rare on both PLDs, which makes a statistically reliable determination of their surface age or resurfacing rate difficult. The rarity and small size of PLD craters means the surface layers are obviously much younger than the surrounding deposits. However, this offers little constraint on how much older the lower strata may be.

Crater counts reveal that the SPLD surface is certainly much older than its northern counterpart. Interpretation of crater counts from Viking data (Herkenhoff & Plaut 2000) indicated a surface age of ∼10 to 20 million years (Myr). Koutnik et al. (2002) used MOLA and MOC data to increase the number of detected craters and thus estimate an age of 30 to 100 Myr. Plaut (2005)

used craters discovered in THEMIS images to derive an age of tens of millions of years. The more recent division of the SPLD into separate stratigraphic units (Kolb & Tanaka 2006, Milkovich & Plaut 2008) complicates matters, as these units had been combined for the purposes of crater counting by studies to date.

The surface of Planum Boreum is much younger. Herkenhoff & Plaut (2000) could find no craters larger than 300 m in the Viking dataset and used that fact to place a 120-thousand-year (Kyr) upper bound on the surface age. Tanaka (2005) used two craters on the layered exposures within NPLD troughs to infer an age of 3.6 Myr (with considerable uncertainty). This could be thought of as dating the formation of the exposing troughs and placing a minimum age on the layers the trough exposes. Craters on the flat intertrough surfaces have been used (Tanaka 2005) to date that surface at only 8.7 Kyr (again with considerable uncertainty), indicating that significant NPLD resurfacing occurred after trough formation. Galla et al. (2008) identified a population of 70 craters on this deposit, the size-frequency distribution of which indicates continuous resurfacing over the period in which these craters accumulated and so precludes a single age estimate.

Deformation

The acquisition of high-resolution topography (Smith et al. 2001) over Planums Boreum and Australe (see **Figure 1**) allows for investigation of the role of ice flow in shaping these deposits. Significant flow could be expected, as the PLDs are ice-rich and timescales compared with the existence of terrestrial ice are long; however, the role of flow on Mars is limited, in comparison to the role of flow on Earth, by the relatively low gravity and cold temperatures. Zuber et al. (1998) used a model that balances outward ice flow with accumulation to explain the observed dome-like shape (**Figure 1**, profile B-B′) of Planum Boreum. Ivanov & Muhleman (2000) modeled the effects of sublimation on Planum Boreum and concluded that sublimation alone could account for the overall shape observed. More recent radar observations (**Figure 3*b***) show that the dome-like shape of Planum Boreum actually comes about only because the NPLD is draped over the smaller basal unit (Phillips et al. 2008), which has a high sand content and is unlikely to have ever flowed. Simulations of an accumulating and flowing Planum Boreum show that flow has a minimal effect on the overall shape of the deposit (Greve & Mahajan 2005). However, analysis of Gemini Lingula, which rests on a flat basement (see **Figure 3*b***), shows that its shape (**Figure 1**, profile A-A′) closely matches that expected from a flowing ice mass (Winebrenner et al. 2008). Winebrenner et al. (2008) propose a two-stage evolution whereby flow initially balances accumulation in setting the shape of Gemina Lingula and is followed by a period in which the effects of flow are negligible and the troughs that currently incise the surface are formed.

The flow rates expected for water ice under martian conditions have been the subject of detailed modeling and vary with climatic fluctuations (Greve 2000, Greve & Mahajan 2005) and impurity concentration (Durham et al. 1997, Greve & Mahajan 2005). The consensus value from many of these studies is that current flow rates in the NPLD are on the order of 0.1–1 mm year^{-1} (Hvidberg 2003; Greve et al. 2003, 2004), although higher rates (centimeters per year) are possible near sloping trough walls. Ice flow near troughs can distort the shape of the strata (Fisher 2000, Hvidberg 2003). Unfortunately, the complicated radar signals returned by the troughs cannot be uniquely interpreted at this time to test for this effect (Phillips et al. 2008). Milkovich et al. (2008a) found local variations in layer orientation that could be due to near-trough flow. However, stratigraphic analysis of NPLD layers and comparison with flow models (Fishbaugh & Hvidberg 2006) do not support a significant role for ice flow within the upper several hundred meters of the deposit. Similarly, the shape of SPLD strata (Byrne & Ivanov 2004) appear to rule out significant flow after trough formation in the upper section of Planum Australe.

Although no landforms unambiguously associated with ice flow have yet been identified, viscous relaxation may have important consequences. Pathare et al. (2005) modeled the effects of viscous relaxation on SPLD craters, showing that this mechanism could explain the observed distribution of crater sizes and depths. In the absence of further ablation, it has been shown that troughs within the NPLD will close due to ice relaxation; however, the rate is sensitive to both the exponent in the law relating stress to strain-rate and ice temperature. Using different values of these parameters, Hvidberg (2003) and Pathare & Paige (2005) derived widely varying trough-closure timescales of 0.1 to a few million years, respectively; thus, the importance of this process cannot be judged without confident knowledge of the thermal history of the ice.

Faults are rare in both PLDs. Offset layers can be observed in the NPLD in the vicinity of Udzha crater (Tanaka 2005). A set of grabens, which occur along the crests of broad ridges, have also been identified on the upper surface of the NPLD. (Nunes et al. 2006, 2007). Tanaka et al. (2008) have mapped eight of these systems, which contain trenches ~100 m across, with lengths up to 23 km, some of which are arranged in echelon patterns. HiRISE data show that the boundaries of these features coincide with strings of rimless pits a few meters across (Byrne et al. 2007, Tanaka et al. 2008). Proposed formation mechanisms include differential stresses due to either viscous flow (Nunes et al. 2006, 2007) or compaction over an irregular substrate (Tanaka et al. 2008). In the SPLD, several isolated faults displaying offset layers are known on the bounding scarp of Ultima Lingula (Murray et al. 2001). The concentration of tectonic activity in this region of the SPLD may result from the local maximum in the thickness (**Figure 1**, profile D-D′) of the deposit (Kolb & Tanaka 2001, Plaut et al. 2007a).

Connection to Climate and Mars's Orbit

Similar precession rates of the martian spin axis and orbit plane lead to a condition near secular spin-orbit resonance, which allows martian obliquity to undergo large variations (Ward 1973) with a period of ~120 Kyr. Obliquity is further modulated by variation of the inclination of the orbit, which occurs with a period of 1200 Kyr. Mars also has a significant nonzero eccentricity, which leads to a pronounced difference in the peak insolation experienced between the poles. The current argument of perihelion causes perihelion passage close to southern summer solstice (L_s 252), leading to short, hot southern summers and longer, cooler northern summers. The argument of perihelion varies with a period of 51 Kyr, whereas the magnitude of the eccentricity varies with periods close to 95 to 99 Kyr and 2400 Kyr (Laskar et al. 2004). **Figure 4** illustrates these variations and their effects on north polar insolation (Laskar et al. 2002).

The evolution of these parameters is chaotic (Laskar & Robutel 1993, Touma & Wisdom 1993); thus, the length of an accurate solution is limited by imprecision in the current precession rates. Recent refinement of these rates by the Pathfinder (Folkner et al. 1997) and MGS (Yoder et al. 2003) missions means that the current best solution (Laskar et al. 2004) is now accurate for 10 to 20 Myr. Ironically, the chaotic nature of these variations allows for confident determination of their statistical behavior. Laskar et al. (2004) find the most probable eccentricity and obliquity over martian history to be 0.068° and 41.8°, respectively. Thus, stable ice at the martian poles may be the exception rather than the rule.

Despite their chaotic nature, a salient feature of all orbital solutions conducted after 1990 is the transition to a substantially higher mean obliquity (see **Figure 4*d***) ~5 Ma (Ward & Rudy 1991; Touma & Wisdom 1993; Laskar et al. 2002, 2004), which appears when general relativistic effects are included in the solution. The associated insolation increase (**Figure 4*f***) could allow the annual ablation of decimeters of ice from the polar deposits, which, in the absence of mitigating effects, would destroy both PLDs in $\sim 10^4$ years (Jakosky et al. 1995; Mischna et al. 2003;

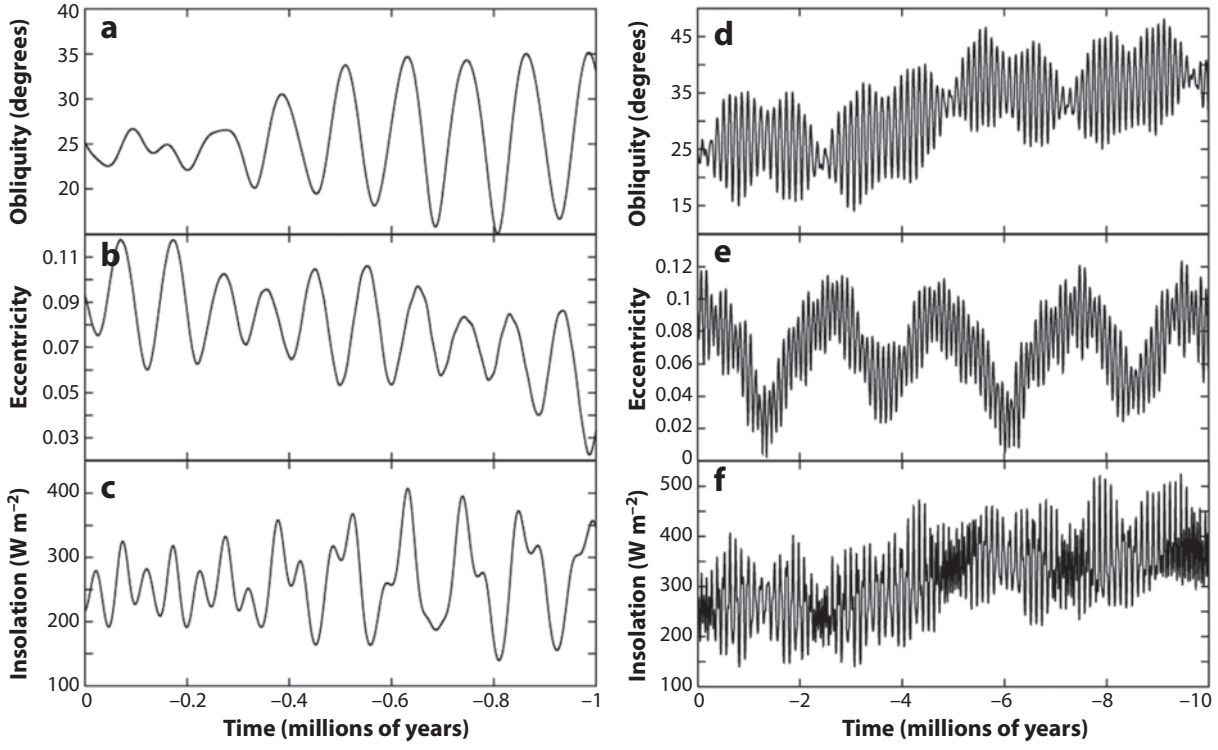

Figure 4

Variation of obliquity, eccentricity, and north polar insolation over timescales of 1 and 10 Myr, as calculated by Laskar et al. (2002). Adapted with permission from Macmillan Publishers Ltd: *Nature* (Laskar et al. 2002), copyright 2002.

Levrard et al. 2004, 2007; Forget et al. 2006). Although it is entirely possible that the bulk of the NPLD are younger than this high-obliquity epoch, the cratering record of the SPLD suggests a surface at least 10^7 years old (Herkenhoff & Plaut 2000, Koutnik et al. 2002). This apparent contradiction may be explained if the sublimation of water ice is a self-limiting process. Dust within the PLD may accumulate on its surface as a lag, when the volatile water ice is removed, and may retard sublimation of the underlying ice when thick enough. However, the details of the effect of dust lags on the sublimation rate are not well understood. Levrard et al. (2007) attempted to model the effects of dust lags by assuming a lag thicker than one meter would lead to a 10-fold reduction in sublimation, whereas thinner dust layers would have no effect; however, in their simulations, even lags this efficient did not allow the survival of the NPLD previous to 4 Ma.

Some studies have attempted to detect periodicities in the PLD stratigraphy that can be related to the orbital periodicities discussed above. Laskar et al. (2002) combined MOLA data with brightness variations in a MOC image of NPLD stratigraphy to construct a virtual core of brightness versus depth. They correlated this with a record of polar insolation versus time (**Figure 4*c***) and found that a deposition rate of 0.05 cm year^{-1} produced the best match for the uppermost 250 m of NPLD stratigraphy. Their spectral analysis uncovered a dominant signal in brightness variation with depth with a wavelength of ~26 m, which they associated with the precession of the argument-of-perihelion timescale (51 Kyr). Milkovich & Head (2005) performed a spectral analysis on 13 similarly assembled virtual cores in widely spaced locations over the NPLD [later expanded by Milkovich et al. (2008a)]. The dominant wavelengths they derived for the uppermost

300 m of NPLD stratigraphy ranged from 23 to 35 m, with a median of 29 m. They likewise interpreted this signal as related to the precession of the argument of perihelion. These studies agree that ~10 cycles ~25–30 m in wavelength dominate the stratigraphy of the upper 250–300 m. Below this depth, however, Milkovich & Head (2005) argued for a 100 m–thick zone with no detectable signal, whereas Laskar et al. (2002) argued that stratigraphy within this zone could be matched to the insolation record with a lower accumulation rate. Milkovich & Head (2005) also probed deeper into the NPLD stratigraphy, arguing for a third (with a dominant signal of 35 m) and a fourth (multiple dominant signals) stratigraphic zone at depths of 400 to 600 m and 600 to 800 m, respectively. Perron & Huybers (2008) assembled 30 similar virtual cores and performed spectral and wavelet analysis to search for periodicities and localized periodicities in NPLD stratigraphy. They uncovered signals with wavelengths of 1 to 3 m and, more weakly, in the 20 to 80 m range; however, in many cases, they found that the stratigraphic spectra differ little from those that a stochastic process would generate. To date, this type of analysis been applied almost exclusively to the NPLD. Milkovich et al. (2008a) applied this method to a single exposure of the SPLD and detected a dominant stratigraphic wavelength of 35 m.

Despite the success of these studies, they contain an unavoidable limitation. It is not clear that the brightness of a layer exposure is representative of the properties of the layer. HiRISE data have shown (Herkenhoff et al. 2007, Fishbaugh et al. 2008b) that the NPLD trough walls are covered with a lag deposit that can be seen slumping downslope in several locations. Brightness variations are related to slope and texture of the lag, which may or may not correspond uniquely with the properties of the layer it covers. These data also show that decimeter patches of frost are common, which, in lower resolution imaging data (such as MOC), will not be resolved and will raise the apparent brightness of layer exposures. In an effort to avoid this problem, Fishbaugh et al. (2008b) analyzed HiRISE image data in conjunction with a high-resolution DEM created from a HiRISE stereo pair. Rather than using the layer brightness, they used morphologic criteria to designate certain layers as marker beds and examined their spacing (20–30 m) in addition to the spacing of the thinner intervening layers (~1 m). The ratio of these wavelengths is close to that of the periodicities of inclination and argument of perihelion, which implies an accumulation rate ~30 times slower than the rate Laskar et al. (2002) and Milkovich & Head (2005) have derived.

Recent radar observations of NPLD stratigraphy (Phillips et al. 2008) reveal four finely layered packages separated by homogeneous regions (**Figure 3*b***). Phillips et al. (2008) interpret the radar reflections as dust-rich layers and the homogeneous regions as relatively dust poor. They suggest that episodes of high obliquity and eccentricity may generate the dusty meteorology necessary to deposit dust-rich layers and vice versa. SHARAD shows fine layering in the uppermost 500 m of the NPLD; if the first homogeneous region relates to the most recent low in obliquity (~800 Kya), then the average accumulation in each argument of perihelion cycle (51 Kyr) is ~32 m, i.e., very similar to the results of Laskar et al. (2002) and Milkovich & Head (2005).

Lower Latitude Ice and Martian "Ice Ages"

Ice on Mars is not confined to the poles and, although the focus of this article is on the polar deposits, discoveries over the past few years mean that it is now impossible to discuss the polar deposits in isolation. The gamma-ray and neutron spectrometers aboard the M01 spacecraft have demonstrated that the top meter of the high-latitude regolith is rich in water ice (Boynton et al. 2002, Feldman et al. 2002, Mitrofanov et al. 2002). A suite of geomorphologic features, such as viscous flow features (Milliken et al. 2003), lobate debris aprons (Pierce & Crown 2003), a dissected mantle deposit (Mustard et al. 2001), latitude-dependent topographic statistics (Kreslavsky & Head 2000, 2002), and recently formed gullies (Malin & Edgett 2000, Milliken et al. 2003) in

the latitude range of 30° to 60°, point to the presence and current retreat of a pervasive ice-rich mantle. Geomorphic studies of the flanks of the high-elevation Tharsis Montes and Olympus Mons at equatorial latitudes suggest that kilometer-thick glaciers may have formed there over the past 100 Myr (Head & Marchant 2003; Milkovich et al. 2006; Shean et al. 2005, 2007) and have since disappeared.

Theoretical studies have suggested that the polar deposits can lose large amounts of material during episodes of high obliquity (Jakosky et al. 1995; Mischna et al. 2003; Levrard et al. 2004, 2007; Forget et al. 2006), which will be redeposited in the midlatitudes and the Tropics, with preferential deposition in areas of high thermal inertia or elevation (Mischna et al. 2003).

On the basis of these observational and theoretical results, Head et al. (2003) postulated that Mars may recently have undergone an "ice age," during which water ice was transported from the polar deposits to latitudes potentially as low as 30°. In this model, mid-latitude ice is deposited with admixed dust when obliquity exceeds 30° (as happened regularly 400–2100 Kyr ago; **Figure 4*d***) and is removed, leaving a friable lag deposit, when obliquity ranges from 20° to 30° (the current situation). Ice at latitudes higher than ~60° is currently stable (Mellon & Jakosky 1995), as indicated by gamma-ray and neutron spectrometer results, whereas the mid-latitude geomorphologic evidence mentioned above corresponds to deposits in the process of removal, the upper meter of which is already largely desiccated. Analysis of ground-ice stability over the past five million years suggests roughly 40 such "ice ages" may have occurred (Schorghofer 2007).

Modeling of these processes with general circulation models suggests that polar ice would be transported only to high-elevation equatorial areas (e.g., Tharsis Montes) under high obliquity. Later, when obliquity is lower, these equatorial deposits would be transported back to the mid- and high latitudes with a distribution dependent on how low the obliquity is (Levrard et al. 2004, 2007; Forget et al. 2006). Although most of these models only investigate the role of the NPLD as a water source, Forget et al. (2006) also considered the role of the SPLD as an ice reservoir. They found substantial accumulation of ice east of Hellas, a region that currently sports tens of lobate debris aprons now known to be composed of almost pure ice (Holt et al. 2008, Plaut et al. 2008).

Geomorphologic and theoretical studies are converging to paint a picture in which kilometer-thick reservoirs of water ice can move from pole to equator in response to orbital change. The current low obliquity and lack of an equatorial water source mean that mid-latitude ice is in the process of being transported poleward and that the NPLD is likely growing today. A little investigated question is how the SPLD accumulated, given that the topographic asymmetry between the poles consistently favors north polar ice accumulation (Richardson & Wilson 2002) and that the crater record shows these deposits have survived many obliquity cycles. Montmessin et al. (2007) show that SPLD accumulation occurs (at the expense of the NPLD) when perihelion coincides with northern summer at times of low obliquity. However, this effect is weak and capable of transporting only a few meters of ice in each cycle.

OLDER POLAR DEPOSITS

Dorsa Argentea Formation

The Dorsa Argentea Formation (DAF) gets its name from the sinuous ridges (the Dorsa Argentea) that cross its surface. The DAF is Hesperian in age and forms plains next to and beneath Planum Australe (Tanaka & Scott 1987) in the area indicated in **Figure 1**. The DAF extends equatorward hundreds of kilometers from the periphery of the SPLD, from longitudes of –100° to +30°E, and covers the floor of the Prometheus impact basin (**Figure 1**). Geologic mapping also suggests

that the DAF extensively underlies the SPLD, with outcrops in Promethei Chasma and Ultimum Chasma (Tanaka & Kolb 2001, Kolb & Tanaka 2006).

Analysis of MGS imaging and topography data suggests that this deposit may be the devolatilized remnant of an ancient polar ice sheet (Head & Pratt 2001). Head & Pratt (2001) suggest that this ice sheet melted rather than sublimed and that the sinuous ridges of the DAF are eskers, although there are alternate formation theories invoking inverted-relief channel deposits (Tanaka & Kolb 2001). Analysis of flat-topped edifices within the margins of the DAF (Ghatan & Head 2002) suggests that they may have formed as subglacial volcanoes, which could have provided the thermal impetus for a regional meltback event. Drainage channels at the eastern margin of the DAF (Milkovich et al. 2002) indicate that meltwater drained from crater to crater, overtopping each in turn and finally emptying into the Prometheus impact basin. Channels leading away (downhill) from the western margin of the DAF suggest that meltwater traveled up to 1600 km equatorward, emptying into the Argyre basin (Ghatan & Head 2004).

MARSIS has detected an extensive subsurface reflection in terrain surrounding Planum Australe, and the extent of this reflection closely matches the extent of the DAF (Plaut et al. 2007b). The depth to the subsurface echo depends on the composition of the DAF materials, but it is in the range of 600 to 900 m (for basaltic to icy compositions). The radar transparency data are consistent with a substantial fraction of ice in this upper few hundred meters.

North Polar Basal Unit and Circumpolar Dunes

The BU lies stratigraphically between the NPLD and the Vastitas Borealis Formation (**Figure 3*b***) and was first observed in MGS imaging and topographic data (Kolb & Tanaka 2001, Byrne & Murray 2002, Edgett et al. 2003, Fishbaugh & Head 2005). Although almost entirely buried by the NPLD, this unit could be identified by exposures located mostly at the head scarps of Chasma Boreale and in the Olympia Cavi (**Figure 1**, profile A-A′).

Exposures of the BU (shown in **Figure 3*c*,*iii***; **Figure 5**) are associated with nearby sand dunes, and erosion of this unit is providing the sand-sized material that supplies the current circumpolar dune fields (Byrne & Murray 2002, Fishbaugh & Head 2005). Detailed geologic mapping now shows that the BU has two components separated by a major unconformity, the lower Rupes Tenuis unit (early Amazonian age) and the upper Planum Boreum Cavi unit (middle Amazonian) (Tanaka et al. 2008), with the sandy material being concentrated in the Planum Boreum Cavi unit. Original analysis of BU-NPLD contact elevations suggested that Olympia Planum (**Figure 1**, profile A-A′) is primarily composed of the BU and that the BU was absent beneath the NPLD in Gemina Lingula (Byrne & Murray 2002, Fishbaugh & Head 2005). **Figure 3*b*** shows this is largely confirmed by SHARAD data (Phillips et al. 2008); however, the unit appears discontinuous at the transition between the main dome of Planum Boreum and Olympia Planum. Mapping by Tanaka et al. (2008) suggests that the BU beneath Olympia Planum is dominated by the Planum Boreum Cavi unit, whereas the BU under Planum Boreum is dominated by the Rupes Tenuis unit. This transition may explain the BU's lack of continuity in the radar data at this location.

HiRISE data (e.g., **Figure 5**) show that the Planum Boreum Cavi unit is made up of interbedded icy and dark layers (Herkenhoff et al. 2007, Tanaka et al. 2008). Cross-bedding observed within the dark layers indicates that they are composed of weakly cemented sand (Herkenhoff et al. 2007). The icy layers exhibit pervasive polygonal fracturing and are being undercut by removal of sand from darker layers. Active mass-wasting of these icy polygonal blocks (a few meters in size) in response to this undercutting has been observed (Russell et al. 2008). The Planum Boreum Cavi unit appears to have formed from episodes of polar ice deposition that alternated with migration of sand sheets over the polar deposits. The lower layers in the NPLD exhibit the same polygonal

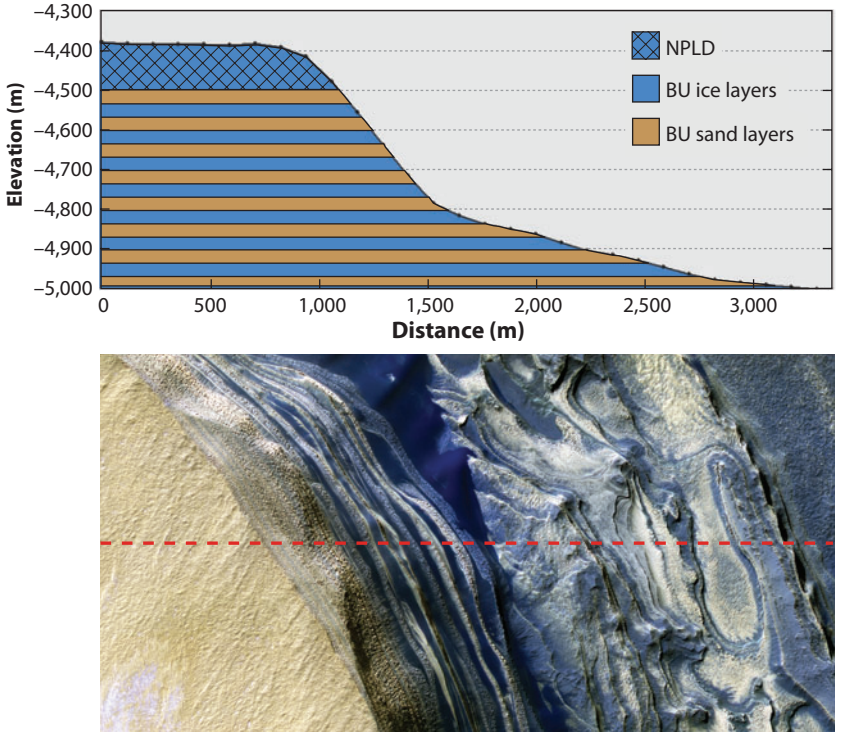

Figure 5

The lower panel is the HiRISE false-color image PSP_001334_2645, at 343°E 84.4°N, showing an exposure of the north polar layered deposits (NPLD) and the basal unit (BU) at the head of Chasma Boreale. The upper panel shows a MOLA elevation profile through the center of the image (*dashed red line*), with the BU and NPLD units also indicated.

fracturing (**Figure 5**), leading Herkenhoff et al. (2007) to argue that deposition of the BU and NPLD was continuous, with the only difference being that the sand supply was exhausted during deposition of the NPLD. Sand eroded from the BU has formed several extensive dunefields that are loosely connected to form a circumpolar sand sea. At least some dunes in the circumpolar sand sea appear to be currently active (Bourke et al. 2008).

Olympia Planum is almost completely covered by the Olympia Undae dunefield, dominated by transverse dunes, although patches of the underlying BU can be seen in the interdune areas. Olympia Undae is unusual in two major respects: First, the thermal inertia of these dunes is much lower (25–150 in MKS units) than dunefields elsewhere on Mars (Paige et al. 1994, Herkenhoff & Vasavada 1999). Previous authors attributed this to the sand grains being composed of agglomerates of dust eroded from the NPLD. However, cross-bedding with the BU shows that this material was not deposited as dust. These thermal inertia measurements remain, for now, unexplained. The second unusual property of this dunefield is the large concentration of the mineral gypsum, discovered in the eastern half by OMEGA (Langevin et al. 2005a) and which decreases as one moves westward. This distribution is consistent with transport of material from east to west, as gypsum is a relatively soft mineral and will likely get broken down to removable dust by saltation. Despite being the main source of the dune material, the BU does not show a gypsum spectral signature (Fishbaugh et al. 2007). CRISM data show that gypsum is more concentrated along the crests of dunes than in the interdune hollows (Roach et al. 2007).

Gypsum requires liquid water to form; thus, its presence requires circumstances very different than today's martian environment. The facts that gypsum is easily destroyed by saltation and that this dunefield is active today (Bourke et al. 2008) suggest that the presence of gypsum is due to an ongoing or recent process; however, the activity seen by Bourke et al. (2008) was far from the gypsum-rich area and may not be an indication that current saltation is widespread. Fishbaugh et al. (2007) suggested that meltwater escaped from beneath Planum Boreum and percolated through the dunes, directly altering minerals to gypsum. Tanaka (2006) suggested that hydrothermal activity in grabens radiating from Alba Patera formed the gypsum and that it has been recently exhumed.

DISCUSSION

The past decade of exploration has shown the martian polar deposits to be wonderfully complex; however, the original basic premise that the PLDs are domes of dusty water ice that record recent climate is still sound. High-resolution imagery, subsurface radar sounding of internal layers, hyperspectral data, better orbital solutions, and general circulation models mean we can investigate the connection between orbital elements, climate, the residual caps, and PLD stratigraphy in considerable detail. Analysis of the MRO datasets is still in the early stages and the upcoming few years will doubtless witness a host of new discoveries. Likewise, the data from the recent Phoenix mission will certainly shed light on the exchange of ice between the high latitudes and the polar deposits. Today's main sticking points are described below as future issues. We can expect considerable progress on these issues over the next five years. The reader is referred to Fishbaugh et al. (2008a) for a comprehensive list of open issues in Mars polar science.

Despite the progress described in this review and the work still to be done on the MRO dataset, we already see some of the limitations of studying these deposits purely through orbital remote sensing, e.g., the mantling deposit on north polar troughs places a limit on our study of the layers exposed there, which no increase in resolution will overcome. Earth's ice sheets are a treasure trove of climatic records; however, this information has been liberated primarily through physical analysis of ice cores. In the long term, in situ analysis of polar samples from a range of depths will be required for a full understanding of the martian polar deposits and their climatic record.

SUMMARY POINTS

1. The residual ice caps appear currently stable in extent, and the observed changes in the NRIC are reversible on a timescale of 1 to 2 martian years. Observations suggest that the SRIC has recently retreated to its current size, although this event cannot be dated. Both residual caps are thin, on the order of 1 m for the NRIC and a few meters for the SRIC. The SRIC is not a significant reservoir of CO_2, totaling less than a few percent of the current atmosphere.
2. Researchers have observed active landscape evolution through sublimation of CO_2 on the SRIC, although the volume of the cap may still be stable or even increasing. Therefore, such evolution is not evidence for secular climate change. Grain sizes deduced from spectral observations of the NRIC imply exposure of old ice and thus net ablation, although its thin nature implies that this situation cannot persist for long.

3. The PLDs are stratified domes up to 3 to 4 km thick and are predominantly composed of water ice. Radar transparency indicates a dust concentration of less than 10%, although SPLD density derived from gravity data suggests 15%. Basal melting appears not to occur in the current environment. Despite the icy composition of the PLDs, studies to date indicate that flow is likely to have played a minor role in recent history.
4. Climate change caused by orbital variations transported large portions of the PLDs to sites in the equatorial region and mid-latitudes during the Amazonian period. Good agreement exists between simulations and geomorphologic observations concerning the locations of these nonpolar sites.
5. Interpretation of the Dorsa Argentea Formation and the north polar basal unit imply that large domes of PLD have not been a stable feature of the martian landscape throughout its history, which is consistent with independent theoretical work that indicates that the mean obliquity of Mars over its history exceeds 40°.

FUTURE ISSUES

1. Better constraints on surface meteorology over the residual ice caps are required, especially on radiative energy balance and atmospheric water vapor, to address questions of present-day mass balance. A longer spacecraft observational record is required to more fully characterize interannual meteorological variability and its effect on ice stability. Modeling suggests that SRIC evolution is especially sensitive to global dust storms, and this interannual variability may be recorded in the layers of that deposit.
2. The connection between climate and the properties of the polar layers remains uncertain. What observable properties of the current layers can be related to the climatic conditions that prevailed during their formation, and is this relationship unique? Modeling of dust-storm activity and ice temperatures in past climates is needed to link layer properties to climatic conditions.
3. Most of the modeling of the exchange of material between the poles and the Tropics has focused on the NPLD over the past 5 Myr; however, the SPLD has been stable for tens of millions of years. How does the history of the SPLD fit into this picture? How can the SPLD be larger and more stable than the NPLD when they are compositionally similar and the polar topographic asymmetry consistently favors north polar deposition?
4. The role of lag deposits in stabilizing the PLD has, for the most part, been treated very simplistically, but this is likely the key to understanding how much material may have been transported from polar to tropical reservoirs. Further investigation of this effect and its incorporation into general circulation models is needed.

DISCLOSURE STATEMENT

The author is not aware of any biases that might be perceived as affecting the objectivity of this review.

ACKNOWLEDGMENTS

Thanks are due to Professor Bruce Murray of the California Institute of Technology for inspiring a career that keeps me out of trouble. I'm grateful for the helpful comments on the text provided by Kate Fishbaugh, Ken Herkenhoff, Sarah Milkovich, Asmin Pathare, Patrick Russell, Jim Skinner, Ken Tanaka, Tim Titus, and Dale Winebrenner.

LITERATURE CITED

Aharonson O, Zuber MT, Rothman DH. 2001. Statistics of Mars' topography from the Mars Orbiter Laser Altimeter: Slopes, correlations, and physical models. *J. Geophys. Res.* 106:23723–36

Aharonson O, Zuber MT, Smith DE, Neumann GA, Feldman WC, et al. 2004. Depth, distribution, and density of CO_2 deposition on Mars. *J. Geophys. Res.* 109:5004

Anguita F, Babin R, Benito G, Gomez D, Collado A, et al. 2000. Chasma Australe, Mars: Structural framework for a catastrophic outflow origin. *Icarus* 144:302–12

Barker ES, Schorn RA, Woszczyk A, Tull RG, Little SJ. 1970. Mars: Detection of atmospheric water vapor during the southern hemisphere spring and summer season. *Science* 170:1308–10

Benito G, Mediavilla F, Fernández M, Márquez A, Martinez J, et al. 1997. Chasma Boreale, Mars: A sapping and outflow channel with a tectono-thermal origin. *Icarus* 129:528–38

Bibring J-P, Langevin Y, Gendrin A, Gondet B, Poulet F, et al. 2005. Mars surface diversity as revealed by the OMEGA/Mars express observations. *Science* 307:1576–81

Bibring J-P, Langevin Y, Poulet F, Gendrin A, Gondet B, et al. 2004. Perennial water ice identified in the south polar cap of Mars. *Nature* 428:627–30

Bonev BP, Hansen GB, Glenar DA, James PB, Bjorkman JE. 2008. Albedo models for the residual south polar cap on Mars: Implications for the stability of the cap under near-perihelion global dust storm conditions. *Planet. Space Sci.* 56:181–93

Bourke MC, Edgett KS, Cantor BA. 2008. Recent aeolian dune change on Mars. *Geomorphology* 94:247–55

Boynton WV, Feldman WC, Squyres SW, Prettyman TH, Bruckner J, et al. 2002. Distribution of hydrogen in the near surface of Mars: Evidence for subsurface ice deposits. *Science* 297:81–85

Byrne S, Herkenhoff KE, Russell P, Hansen C, McEwen A, et al. 2007. *Preliminary HiRISE polar geology results*. Presented at Lunar Planet. Sci. Conf., 38th, Abstr. 1930

Byrne S, Ingersoll AP. 2003a. A sublimation model for Martian south polar ice features. *Science* 299:1051–1053

Byrne S, Ingersoll AP. 2003b. Martian climatic events on timescales of centuries: Evidence from feature morphology in the residual south polar ice cap. *Geophys. Res. Lett.* 30:1696

Byrne S, Ivanov AB. 2004. Internal structure of the Martian south polar layered deposits. *J. Geophys. Res.* 109:11001

Byrne S, Murray BC. 2002. North polar stratigraphy and the paleo-erg of Mars. *J. Geophys. Res.* 107:5044

Byrne S, Russell PS, Fishbaugh KE, Hansen CJ, Herkenhoff KE, et al. 2008a. *Explaining the persistence of the Southern Residual Cap of Mars: HiRISE data and landscape evolution models*. Presented at Lunar Planet. Sci. Conf., 39th, Abstr. 2252

Byrne S, Zuber MT, Neumann GA. 2008b. Interannual and seasonal behavior of Martian residual ice-cap albedo. *Planet. Space Sci.* 56:194–211

Calvin WM, Titus TN. 2008. Summer season variability of the north residual cap of Mars as observed by the Mars Global Surveyor Thermal Emission Spectrometer (MGS-TES). *Planet. Space Sci.* 56:212–26

Christensen PR, Bandfield JL, Hamilton VE, Ruff SW, Kieffer HH, et al. 2001. Mars Global Surveyor Thermal Emission Spectrometer experiment: Investigation description and surface science results. *J. Geophys. Res.* 106:23823–72

Christensen PR, Jakosky BM, Kieffer HH, Malin MC, McSween HY Jr, et al. 2004. The Thermal Emission Imaging System (THEMIS) for the Mars 2001 Odyssey Mission. *Space Sci. Rev.* 110:85–130

Clifford SM. 1987. Polar basal melting on Mars. *J. Geophys. Res.* 92:9135–52

Clifford SM, Crisp D, Fisher DA, Herkenhoff KE, Smrekar SE, et al. 2000. The state and future of Mars polar science and exploration. *Icarus* 144:210–42

Clifford SM, Doran PT, Fisher DA, Herd CDK. 2005. Third Mars polar science special issue: Key questions, needed observations, and recommended investigations. *Icarus* 174:291–93
Clifford SM, Thorsteinsson T, Björnsson H, Fisher DA, Paige DA. 2001. Introduction to the second Mars polar science special issue. *Icarus* 154:1–2
Cutts JA. 1973. Nature and origin of layered deposits of the Martian polar region. *J. Geophys. Res.* 78:4231–49
Durham WB, Kirby SH, Stern LA. 1997. Creep of water ices at planetary conditions: A compilation. *J. Geophys. Res.* 102:16293–302
Edgett KS, Williams RME, Malin MC, Cantor BA, Thomas PC. 2003. Mars landscape evolution: influence of stratigraphy on geomorphology in the north polar region. *Geomorphology* 52:289–97
Feldman WC, Boynton WV, Tokar RL, Prettyman TH, Gasnault O, et al. 2002. Global distribution of neutrons from Mars: Results from Mars odyssey. *Science* 297:75–78
Fishbaugh KE, Byrne S, Herkenhoff KE, Russell PS, Kirk RL, et al. 2008b. *Characterizing and defining layers in the Martian North Polar deposits using HiRISE: Implications for climate change*. Presented at Lunar Planet. Sci. Conf., 39th, Abstr. 1781
Fishbaugh KE, Head JW. 2002. Chasma Boreale, Mars: Topographic characterization from Mars Orbiter Laser Altimeter data and implications for mechanisms of formation. *J. Geophys. Res.* 107:5013
Fishbaugh KE, Head JW. 2005. Origin and characteristics of the Mars north polar basal unit and implications for polar geologic history. *Icarus* 174:444–74
Fishbaugh KE, Hvidberg CS. 2006. Martian north polar layered deposits stratigraphy: Implications for accumulation rates and flow. *J. Geophys. Res.* 111:6012
Fishbaugh KE, Hvidberg CS, Beaty D, Clifford S, Fisher D, et al. 2008a. Introduction to the 4th Mars Polar Science and Exploration Conference special issue: Five top questions in Mars polar science. *Icarus* 196:305–17
Fishbaugh KE, Poulet F, Chevrier V, Langevin Y, Bibring J-P. 2007. On the origin of gypsum in the Mars north polar region. *J. Geophys. Res.* 112:7002
Fisher DA. 1993. If Martian ice caps flow—Ablation mechanisms and appearance. *Icarus* 105:501
Fisher DA. 2000. Internal layers in an "accublation" ice cap: A test for flow. *Icarus* 144:289–94
Folkner WM, Yoder CF, Yuan DN, Standish EM, Preston RA. 1997. Interior structure and seasonal mass redistribution of Mars from radio tracking of Mars pathfinder. *Science* 278:1749
Forget F, Haberle RM, Montmessin F, Levrard B, Head JW. 2006. Formation of glaciers on Mars by atmospheric precipitation at high obliquity. *Science* 311:368–71
Galla K, Byrne S, Murray BC, McEwen A, The HiRISE Team. 2008. *Craters and resurfacing of the martian north polar cap*. Presented at Am. Geophys. Union Fall Meet., Abstr 1360
Garvin JB, Sakimoto SEH, Frawley JJ, Schnetzler CC, Wright HM. 2000. Note: Topographic evidence for geologically recent near-polar volcanism on Mars. *Icarus* 145:648–52
Ghatan GJ, Head JW. 2002. Candidate subglacial volcanoes in the south polar region of Mars: Morphology, morphometry, and eruption conditions. *J. Geophys. Res.* 107:5048
Ghatan GJ, Head JW. 2004. Regional drainage of meltwater beneath a Hesperian-aged south circumpolar ice sheet on Mars. *J. Geophys. Res.* 109:7006
Greve R. 2000. Waxing and waning of the perennial north polar H_2O ice cap of Mars over obliquity cycles. *Icarus* 144:419–31
Greve R. 2008. Scenarios for the formation of Chasma Boreale, Mars. *Icarus* 196:359–67
Greve R, Klemann V, Wolf D. 2003. Ice flow and isostasy of the north polar cap of Mars. *Planet. Space Sci.* 51:193–204
Greve R, Mahajan RA. 2005. Influence of ice rheology and dust content on the dynamics of the north-polar cap of Mars. *Icarus* 174:475–85
Greve R, Mahajan RA, Segschneider J, Grieger B. 2004. Evolution of the north-polar cap of Mars: a modeling study. *Planet. Space Sci.* 52:775–87
Haberle RM, Mattingly B, Titus TN. 2004. Reconciling different observations of the CO_2 ice mass loading of the Martian north polar cap. *Geophys. Res. Lett.* 31:5702
Hale AS, Bass DS, Tamppari LK. 2005. Monitoring the perennial martian northern polar cap with MGS MOC. *Icarus* 174:502–12

Hansen G, Giuranna M, Formisano V, Fonti S, Grassi D, et al. 2005. PFS-MEX observation of ices in the residual south polar cap of Mars. *Planet. Space Sci.* 53:1089–1095

Head JW, Marchant DR. 2003. Cold-based mountain glaciers on Mars: Western Arsia Mons. *Geology* 31:641

Head JW, Mustard JF, Kreslavsky MA, Milliken RE, Marchant DR. 2003. Recent ice ages on Mars. *Nature* 426:797–802

Head JW, Pratt S. 2001. Extensive Hesperian-aged south polar ice sheet on Mars: Evidence for massive melting and retreat, and lateral flow and ponding of meltwater. *J. Geophys. Res.* 106:12275–300

Herkenhoff KE, Byrne S, Russell PS, Fishbaugh KE, McEwen AS. 2007. Meter-scale morphology of the north polar region of Mars. *Science* 317:1711

Herkenhoff KE, Plaut JJ. 2000. Surface ages and resurfacing rates of the polar layered deposits on Mars. *Icarus* 144:243–53

Herkenhoff KE, Soderblom LA, Kirk RL. 2002. *MOC photoclinometry of the North Polar Residual Cap on Mars*. Presented at Lunar Planet. Sci. Conf., 33rd, Abstr. 1714

Herkenhoff KE, Vasavada AR. 1999. Dark material in the polar layered deposits and dunes on Mars. *J. Geophys. Res.* 104:16487–500

Hofstadter MD, Murray BC. 1990. Ice sublimation and rheology—Implications for the Martian polar layered deposits. *Icarus* 84:352–61

Holt JW, Safaeinili A, Plaut JJ, Head JW, Phillips RJ, et al. 2008. Radar sounding evidence for buried glaciers in the southern mid-latitudes of Mars. *Science* 322:1235–38

Howard AD. 1978. Origin of the stepped topography of the Martian poles. *Icarus* 34:581–99

Howard AD. 2000. The role of Eolian processes in forming surface features of the Martian polar layered deposits. *Icarus* 144:267–88

Howard AD, Cutts JA, Blasius KR. 1982. Stratigraphic relationships within Martian polar cap deposits. *Icarus* 50:161–215

Hvidberg CS. 2003. Relationship between topography and flow in the north polar cap of Mars. *Ann. Glaciol.* 37:363–69

Ivanov AB, Muhleman DO. 2000. The role of sublimation for the formation of the northern ice cap: Results from the Mars orbiter laser altimeter. *Icarus* 144:436–48

Jakosky BM, Haberle RM. 1990. Year-to-year instability of the Mars south polar cap. *J. Geophys. Res.* 95:1359–65

Jakosky BM, Henderson BG, Mellon MT. 1995. Chaotic obliquity and the nature of the Martian climate. *J. Geophys. Res.* 100:1579–84

James PB, Thomas PC, Wolff MJ, Bonev BP. 2007. MOC observations of four Mars year variations in the south polar residual cap of Mars. *Icarus* 192:318–26

Kieffer HH. 1979. Mars south polar spring and summer temperatures—A residual CO_2 frost. *J. Geophys. Res.* 84:8263–88

Kieffer HH. 1990. H_2O grain size and the amount of dust in Mars' residual north polar CAP. *J. Geophys. Res.* 95:1481–93

Kieffer HH. 2000. *Annual punctuated CO_2 slab-ice and jets on Mars*. Presented at 2nd Int. Conf., Mars Polar Sci. Explor., Reykjavík, Iceland

Kieffer HH. 2007. Cold jets in the Martian polar caps. *J. Geophys. Res.* 112:8005

Kieffer HH, Christensen PR, Titus TN. 2006. CO_2 jets formed by sublimation beneath translucent slab ice in Mars' seasonal south polar ice cap. *Nature* 442:793–96

Kieffer HH, Martin TZ, Chase SC Jr, Miner ED, Palluconi FD. 1976. Martian north pole summer temperatures—Dirty water ice. *Science* 194:1341–44

Kieffer HH, Titus TN. 2001. TES mapping of Mars' north seasonal cap. *Icarus* 154:162–80

Kolb EJ, Tanaka KL. 2001. Geologic history of the polar regions of Mars based on Mars global surveyor data. II. Amazonian period. *Icarus* 154:22–39

Kolb EJ, Tanaka KL. 2006. Accumulation and erosion of south polar layered deposits in the Promethei Lingula region, Planum Australe, Mars. *MARS* 2:1–9

Koutnik M, Byrne S, Murray B. 2002. South polar layered deposits of Mars: The cratering record. *J. Geophys. Res.* 107:5100

Kreslavsky MA, Head JW. 2000. Kilometer-scale roughness of Mars: Results from MOLA data analysis. *J. Geophys. Res.* 105:26695–712
Kreslavsky MA, Head JW III. 2002. Mars: Nature and evolution of young latitude-dependent water-ice-rich mantle. *Geophys. Res. Lett.* 29:1719
Langevin Y, Poulet F, Bibring J-P, Gondet B. 2005a. Sulfates in the north polar region of Mars detected by OMEGA/Mars express. *Science* 307:1584–86
Langevin Y, Poulet F, Bibring J-P, Schmitt B, Douté S, et al. 2005b. Summer evolution of the north polar cap of mars as observed by OMEGA/Mars express. *Science* 307:1581–84
Laskar J, Correia ACM, Gastineau M, Joutel F, Levrard B, et al. 2004. Long term evolution and chaotic diffusion of the insolation quantities of Mars. *Icarus* 170:343–64
Laskar J, Levrard B, Mustard JF. 2002. Orbital forcing of the martian polar layered deposits. *Nature* 419:375–77
Laskar J, Robutel P. 1993. The chaotic obliquity of the planets. *Nature* 361:608–12
Leighton RR, Murray BC. 1966. Behavior of carbon dioxide and other volatiles on Mars. *Science* 153:136–44
Levrard B, Forget F, Montmessin F, Laskar J. 2004. Recent ice-rich deposits formed at high latitudes on Mars by sublimation of unstable equatorial ice during low obliquity. *Nature* 431:1072–1075
Levrard B, Forget F, Montmessin F, Laskar J. 2007. Recent formation and evolution of northern Martian polar layered deposits as inferred from a global climate model. *J. Geophys. Res.* 112:6012
Malin MC, Caplinger MA, Davis SD. 2001. Observational evidence for an active surface reservoir of solid carbon dioxide on Mars. *Science* 294:2146–48
Malin MC, Edgett KS. 2000. Evidence for recent groundwater seepage and surface runoff on Mars. *Science* 288:2330–35
Malin MC, Edgett KS. 2001. Mars Global Surveyor Mars Orbiter Camera: Interplanetary cruise through primary mission. *J. Geophys. Res.* 106:23429–570
McEwen AS, Eliason EM, Bergstrom JW, Bridges NT, Hansen CJ, et al. 2007. Mars Reconnaissance Orbiter's High Resolution Imaging Science Experiment (HiRISE). *J. Geophys. Res.* 112:EO5S02
Mellon MT. 1996. Limits on the CO_2 content of the martian polar deposits. *Icarus* 124:268–79
Mellon MT, Jakosky BM. 1995. The distribution and behavior of Martian ground ice during past and present epochs. *J. Geophys. Res.* 100:3367
Milkovich SM, Head JW III. 2005. North polar cap of Mars: Polar layered deposit characterization and identification of a fundamental climate signal. *J. Geophys. Res.* 110:1005
Milkovich SM, Head JW III, Marchant DR. 2006. Debris-covered piedmont glaciers along the northwest flank of the Olympus Mons scarp: Evidence for low-latitude ice accumulation during the Late Amazonian of Mars. *Icarus* 181:388–407
Milkovich SM, Head JW, Neukum G, HRSC Team. 2008a. Stratigraphic analysis of the northern polar layered deposits of Mars: Implications for recent climate history. *Planet. Space Sci.* 56:266–88
Milkovich SM, Head JW, Pratt S. 2002. Meltback of Hesperian-aged ice-rich deposits near the south pole of Mars: Evidence for drainage channels and lakes. *J. Geophys. Res.* 107:5043
Milkovich SM, Plaut JJ. 2008. Martian south polar layered deposit stratigraphy and implications for accumulation history. *J. Geophys. Res.* 113:6007
Milkovich SM, Plaut JJ, Safaeinili A, Phillips RJ, Seu R, et al. 2008b. *Local and regional stratigraphy of the south polar layered deposits of Mars in radar*. Presented at Lunar Planet. Sci. Conf., 39th, Abstr. 466
Milliken RE, Mustard JF, Goldsby DL. 2003. Viscous flow features on the surface of Mars: Observations from high-resolution Mars Orbiter Camera (MOC) images. *J. Geophys. Res.* 108:5057
Mischna MA, Richardson MI, Wilson RJ, McCleese DJ. 2003. On the orbital forcing of Martian water and CO_2 cycles: A general circulation model study with simplified volatile schemes. *J. Geophys. Res.* 108:5062
Mitrofanov I, Anfimov D, Kozyrev A, Litvak M, Sanin A, et al. 2002. Maps of subsurface hydrogen from the high energy neutron detector, Mars odyssey. *Science* 297:78–81
Montmessin F, Haberle RM, Forget F, Langevin Y, Clancy RT, et al. 2007. On the origin of perennial water ice at the south pole of Mars: A precession-controlled mechanism? *J. Geophys. Res.* 112:8
Murchie S, Arvidson R, Bedini P, Beisser K, Bibring J-P, et al. 2007a. Compact Reconnaissance Imaging Spectrometer for Mars (CRISM) on Mars Reconnaissance Orbiter (MRO). *J. Geophys. Res.* 112:5
Murchie S, CRISM Sci. Eng. Teams. 2007b. *First results from the Compact Reconnaissance Imaging Spectrometer for Mars (CRISM)*. Presented at Lunar Planet. Sci. Conf., 38th, Abstr. 1472

Murray B, Koutnik M, Byrne S, Soderblom L, Herkenhoff K, Tanaka KL. 2001. Preliminary geological assessment of the Northern Edge of Ultimi Lobe, Mars South Polar layered deposits. *Icarus* 154:80–97

Murray BC, Soderblom LA, Cutts JA, Sharp RP, Milton DJ, Leighton RB. 1972. Geological framework of the south polar region of Mars. *Icarus* 17:328–45

Murray BC, Ward WR, Yeung SC. 1973. Periodic insolation variations on Mars. *Science* 180:638–40

Mustard JF, Cooper CD, Rifkin MK. 2001. Evidence for recent climate change on Mars from the identification of youthful near-surface ground ice. *Nature* 412:411–14

Ng FSL, Zuber MT. 2006. Patterning instability on the Mars polar ice caps. *J. Geophys. Res.* 111:2005

Nielsen E. 2004. Mars Express and MARSIS. *Space Sci. Rev.* 111:245–62

Nunes D, Byrne S, Hurwitz D. 2006. *Lineaments in northern Martian polar layered deposits: recent faulting*? Presented at Fall Meet. Am. Geophys. Union, San Francisco

Nunes D, Byrne S, Okubo C. 2007. *Recent deformation in the residual northern polar cap of Mars: A breaking story*. Presented at 7th Int. Conf. Mars, Pasadena, CA

Nunes DC, Phillips RJ. 2006. Radar subsurface mapping of the polar layered deposits on Mars. *J. Geophys. Res.* 111:6

Nye JF, Durham WB, Schenk PM, Moore JM. 2000. The instability of a south polar cap on Mars composed of carbon dioxide. *Icarus* 144:449–55

Paige DA, Bachman JE, Keegan KD. 1994. Thermal and albedo mapping of the polar regions of Mars using Viking thermal mapper observations: 1. North polar region. *J. Geophys. Res.* 99:25959–91

Pathare AV, Paige DA. 2005. The effects of martian orbital variations upon the sublimation and relaxation of north polar troughs and scarps. *Icarus* 174:419–43

Pathare AV, Paige DA, Turtle E. 2005. Viscous relaxation of craters within the martian south polar layered deposits. *Icarus* 174:396–418

Pelletier JD. 2004. How do spiral troughs form on Mars? *Geology* 32:365–67

Perron JT, Huybers P. 2008. *Is there an orbital signal in the polar layered deposits on Mars*? Presented at Lunar Planet. Sci. Conf., 39th, Abstr. 1497

Phillips RJ, Zuber MT, Smrekar SE, Mellon MT, Head JW, et al. 2008. Mars north polar deposits: Stratigraphy, age, and geodynamical response. *Science* 320:1182–85

Picardi G, Plaut JJ, Biccari D, Bombaci O, Calabrese D, et al. 2005. Radar soundings of the subsurface of Mars. *Science* 310:1925–28

Pierce TL, Crown DA. 2003. Morphologic and topographic analyses of debris aprons in the eastern Hellas region, Mars. *Icarus* 163:46–65

Piqueux S, Christensen PR. 2008. Deposition of CO_2 and erosion of the Martian south perennial cap between 1972 and 2004: Implications for current climate change. *J. Geophys. Res.* 113:2006

Plaut JJ. 2005. *An inventory of impact craters on the Martian south polar layered deposits*. Presented at Lunar Planet. Sci. Conf., 36th, Abstr. 2319

Plaut JJ, Ivanov A, Safaeinili A, Milkovich SM, Picardi G, et al. 2007a. *Radar sounding of subsurface layers in the south polar plains of Mars: correlation with the Dorsa Argentea Formation*. Presented at Lunar Planet. Sci. Conf., 38th, Abstr. 2144

Plaut JJ, Picardi G, Safaeinili A, Ivanov AB, Milkovich SM, et al. 2007b. Subsurface radar sounding of the south polar layered deposits of Mars. *Science* 316:92–96

Plaut JJ, Safaeinili A, Holt JW, Phillips RJ, Head J, et al. 2008. Radar evidence for ice in lobate debris aprons in the mid-northern latitudes of Mars. *Geophys. Res. Lett.* In press

Prettyman TH, Feldman WC, Mellon MT, McKinney GW, Boynton WV, et al. 2004. Composition and structure of the Martian surface at high southern latitudes from neutron spectroscopy. *J. Geophys. Res.* 109:5001

Richardson MI, Wilson RJ. 2002. Investigation of the nature and stability of the Martian seasonal water cycle with a general circulation model. *J. Geophys. Res.* 107:5031

Roach LH, Mustard JF, Murchie S, Langevin Y, Bibring J-P, et al. 2007. *CRISM spectral signatures of the North Polar Gypsum Dunes*. Presented at Lunar Planet. Sci. Conf., 38th, Abstr. 1970

Rodriguez JAP, Tanaka KL, Langevin Y, Bourke M, Kargel J, et al. 2007. Recent aeolian erosion and deposition in the north polar plateau of Mars. *Mars* 3:29–41

Russell PS, Byrne S, Herkenhoff KE, Fishbaugh KE, Thomas N, et al. 2008. *Active mass-wasting processes on Mars' north polar scarps discovered by HiRISE*. Presented at Lunar Planet. Sci. Conf., 39th, Abstr. 2313
Schorghofer N. 2007. Dynamics of ice ages on Mars. *Nature* 449:192–94
Seidelmann PK, Abalakin VK, Bursa M, Davies ME, de Bergh C, et al. 2002. Report of the IAU/IAG working group on cartographic coordinates and rotational elements of the planets and satellites: 2000. *Celest. Mech. Dyn. Astron.* 82:83–111
Seu R, Phillips RJ, Alberti G, Biccari D, Bonaventura F, et al. 2007a. Accumulation and erosion of Mars' south polar layered deposits. *Science* 317:1715–18
Seu R, Phillips RJ, Biccari D, Orosei R, Masdea A, et al. 2007b. SHARAD sounding radar on the Mars Reconnaissance Orbiter. *J. Geophys. Res.* 112:5
Shean DE, Head JW, Fastook JL, Marchant DR. 2007. Recent glaciation at high elevations on Arsia Mons, Mars: Implications for the formation and evolution of large tropical mountain glaciers. *J. Geophys. Res.* 112:3004
Shean DE, Head JW, Marchant DR. 2005. Origin and evolution of a cold-based tropical mountain glacier on Mars: The Pavonis Mons fan-shaped deposit. *J. Geophys. Res.* 110:5001
Smith DE, Zuber MT, Frey HV, Garvin JB, Head JW, et al. 2001. Mars Orbiter Laser Altimeter: Experiment summary after the first year of global mapping of Mars. *J. Geophys. Res.* 106:23689–722
Tanaka KL. 2005. Geology and insolation-driven climatic history of Amazonian north polar materials on Mars. *Nature* 437:991–94
Tanaka KL. 2006. *Mars' north polar gypsum: Possible origin related to early Amazonian magmatism at Alba Patera and Aeolian Mining*. Presented at 4th Int. Conf. Mars Polar Sci. Expl., Davos, Switz., p. 8024
Tanaka KL, Kolb EJ. 2001. Geologic history of the polar regions of Mars based on Mars Global Surveyor Data. I. Noachian and Hesperian periods. *Icarus* 154:3–21
Tanaka KL, Rodriguez JAP, Skinner JA, Bourke MC, Fortezzo CM, et al. 2008. North polar region of Mars: Advances in stratigraphy, structure, and erosional modification. *Icarus* 196:318–58
Tanaka KL, Scott DH. 1987. Geologic map of the polar regions of Mars. *U.S. Geol. Surv. Misc. Invest. Ser.*, *Map I-1802-BC*
Thomas PC, Malin MC, Edgett KS, Carr MH, Hartmann WK, et al. 2000. North-south geological differences between the residual polar caps on Mars. *Nature* 404:161–64
Thomas PC, Malin MC, James PB, Cantor BA, Williams RME, et al. 2005. South polar residual cap of Mars: Features, stratigraphy, and changes. *Icarus* 174:535–59
Thomas P, Squyres S, Herkenhoff K, Howard A, Murray B. 1992. Polar deposits of Mars. In *Mars*, ed. HH Kieffer, BM Jakosky, CW Snyder, MS Matthews, 23:767–95. Tucson: Univ. Ariz. Press
Titus TN. 2005. Thermal infrared and visual observations of a water ice lag in the Mars southern summer. *Geophys. Res. Lett.* 32:24204
Titus TN, Calvin WM, Kieffer HH, Langevin Y, Prettyman TH. 2008a. Martian polar processes. In *The Martian Surface: Composition, Mineralogy, and Physical Properties*, ed. JF Bell III, p. 25. New York: Cambridge Univ. Press
Titus TN, Colaprete A, Prettyman TH. 2008b. Introduction to planetary space science special issue: Mars polar processes. *Planet. Space Sci.* 56:147–49
Titus TN, Kieffer HH, Christensen PR. 2003. Exposed water ice discovered near the south pole of Mars. *Science* 299:1048–51
Tokar RL, Elphic RC, Feldman WC, Funsten HO, Moore KR, et al. 2003. Mars odyssey neutron sensing of the south residual polar cap. *Geophys. Res. Lett.* 30:1677
Touma J, Wisdom J. 1993. The chaotic obliquity of Mars. *Science* 259:1294–97
Wagstaff KL, Titus TN, Ivanov AB, Castano R, Bandfield JL. 2008. Observations of the north polar water ice annulus on Mars using THEMIS and TES. *Planet. Space Sci.* 56:256–65
Ward WR. 1973. Large-scale variations in the obliquity of Mars. *Science* 181:260–62
Ward WR, Rudy DJ. 1991. Resonant obliquity of Mars? *Icarus* 94:160–64
Warner NH, Farmer JD. 2008a. Importance of aeolian processes in the origin of the north polar chasmata, Mars. *Icarus* 196:368–84
Warner NH, Farmer JD. 2008b. The origin of conical mounds at the mouth of Chasma Boreale. *J. Geophys. Res.* 113:11008

Wieczorek MA. 2008. Constraints on the composition of the martian south polar cap from gravity and topography. *Icarus* 196:506–17

Winebrenner DP, Koutnik MR, Waddington ED, Pathare AV, Murray BC, et al. 2008. Evidence for ice flow prior to trough formation in the martian north polar layered deposits. *Icarus* 195:90–105

Yoder CF, Konopliv AS, Yuan DN, Standish EM, Folkner WM. 2003. Fluid core size of Mars from detection of the solar tide. *Science* 300:299–303

Zuber MT, Phillips RJ, Andrews-Hanna JC, Asmar SW, Konopliv AS, et al. 2007. Density of Mars' south polar layered deposits. *Science* 317:1718–19

Zuber MT, Smith DE, Solomon SC, Abshire JB, Afzal RS, et al. 1998. Observations of the north polar region of Mars from the Mars orbiter laser altimeter. *Science* 282:2053–60

Annual Review
of Earth and
Planetary Sciences

Volume 37, 2009

Contents

Indexes

Errata

An online log of corrections to *Annual Review of Earth and Planetary Sciences* articles may be found at http://earth.annualreviews.org